PARAMETER-ROBUST ERROR ESTIMATES FOR THE DARCY EQUATIONS

RISHI DAS, HARSHA HUTRIDURGA, AMIYA K. PANI, AND RICARDO RUIZ-BAIER

ABSTRACT. We derive parameter-robust error estimates for the Darcy equations with mixed boundary conditions, drawing on the approach of [BKMT20]. Numerical experiments are presented to support the theoretical results.

1. INTRODUCTION

Scope. Darcy's law is a fundamental equation in hydrogeology and fluid dynamics that describes the flow of a fluid through a porous medium. It is widely used in finite element and finite difference methods to solve complex flow problems in porous media, particularly when dealing with heterogeneous materials or non-linear flow behaviors. Darcy's law has been extended to account for more complicated physical phenomena such as non-Darcian flow, turbulent flow, and anisotropic permeability. One such example is Darcy–Forchheimer model (see, e.g., [DHPRB26]), which is often used when the flow is not laminar, and deviations from Darcy's law occur at higher flow velocities.

Solving multiphysics problems, such as Biot's consolidation problem (see, e.g., [BKMRB21]), the Stokes-Darcy problem ([GOS11]), the Biot-Brinkman problem (see, e.g., [HKK$^+$22]), and other important poroelasticity models, often involves analyzing decomposed subproblems. The Darcy problem, as a single-physics problem, arises frequently in many situations. Additionally, ensuring robust stability analysis of these systems is critical for practical applications. Finding robust solvers for such flow problems in porous media is often based on H(div) preconditioners. The H(div)-based mixed formulation of the Darcy problem is discussed in several works (see, e.g., [BKMT20], etc. Following the techniques outlined in [MW11], efficient block-diagonal preconditioners have been developed in [BKMT20]. Instead of using the traditional flux-pressure pair H(div)-L^2, the approach in [BKMT20] involves weighted spaces of H(div) and L^2. A key question of interest is whether robust Céa estimates and uniform convergence rates can be obtained in these weighted spaces.

In this article, we compute stability estimates in both continuous and discrete setups following the approach of [BBF$^+$13] in parameter-weighted Hilbert spaces. Additionally, we derive error estimates and convergence rates, which are robust with respect to the physical parameter κ, and validate the robustness by implementing these convergence rates. The appropriate choice of weighted spaces naturally leads to robust preconditioners, as demonstrated by the general Riesz mapping techniques in [Kir10], [MW11] and the references therein. The norms corresponding to the pressure space, which is a sum space, are non-trivial to implement. To address this, we leverage the robust preconditioners derived in [BKMT20]. The realization of the numerical discretization and the weighted norms is carried out using the `Gridap` finite element software package [BV20]. We exploit the flexibility of this framework and its compatibility with other packages in the Julia ecosystem, such as `LinearOperators` [OS20], to prototype natural Riesz map preconditioners in the weighted sum space. This approach results in solvers that are robust with respect to the physical parameter κ, the permeability of the material, and the resolution of the mesh, thus facilitating the implementation of the weighted norm in the weighted space.

Outline. The remainder of this section reviews standard facts about weighted Sobolev spaces, relevant notation, and the variational formulation of (1.2). Section 2 provides a brief exposition of abstract saddle point problems. Section 3 focuses on robust stability estimates in the continuous case. In Section 4, we study discrete stability estimates and extend them to derive robust Céa estimates and uniform

2020 *Mathematics Subject Classification.* 65N30, 65N12, 65N15.

Key words and phrases. Mixed finite element methods, parameter-robust stability, robust error estimates.

convergence rates. Finally, Section 5 presents numerical results that support the theoretical arguments In the following, we consider a simplistic mathematical model of the Darcy equation in mixed form inspired by [BKMT20].

Notation and Preliminaries. Let $\Omega \subset \mathbb{R}^d$, $d \in \{2,3\}$, denote a domain bounded with a continuous Lipschitz boundary $\partial\Omega$, on which its outward unit normal is denoted by $\boldsymbol{n}$. For $s \geq 0$ and $r \in [1,+\infty]$, we denote by $\mathrm{L}^r(\Omega)$ and $\mathrm{W}^{s,r}(\Omega)$ the usual Lebesgue and Sobolev spaces endowed with the norms $\|\bullet\|_{0,r,\Omega}$ and $\|\bullet\|_{s,r,\Omega}$, respectively. Note that $\mathrm{W}^{0,r}(\Omega) = \mathrm{L}^r(\Omega)$. If $r = 2$, we write $\mathrm{H}^s(\Omega)$ in place of $\mathrm{W}^{s,2}(\Omega)$ and denote the corresponding norm by $\|\bullet\|_{s,\Omega}$. We denote by $\mathbf{H}$ the vectorial counterpart of a generic scalar functional space H. The inner product $\mathrm{L}^2(\Omega)$ for functions valued as scalar, vector, or tensor is denoted by $(\bullet,\bullet)_{0,\Omega}$. We also recall the Hilbert space $\mathbf{H}(\mathrm{div},\Omega) = \{\boldsymbol{v} \in \mathbf{L}^2(\Omega) : \mathrm{div}\,\boldsymbol{v} \in \mathrm{L}^2(\Omega)\}$ endowed with the norm $\|\boldsymbol{v}\|^2_{\mathrm{div},\Omega} = \|\boldsymbol{v}\|^2_{0,\Omega} + \|\mathrm{div}\,\boldsymbol{v}\|^2_{0,\Omega}$. Often, we use a subscript Γ_i on the functional space to denote that the (appropriate) traces vanish on the part of the boundary $\Gamma_i \subset \partial\Omega$.

For two Banach spaces $(X, \|\bullet\|_X)$ and $(Y, \|\bullet\|_Y)$, we denote by $\mathcal{L}(X,Y)$ the space of bounded linear maps from X to Y. The intersection and sum spaces are

$$X \cap Y = \{v : v \in X \text{ and } v \in Y\}, \quad \text{and} \quad X + Y = \{u + v : u \in X \text{ and } v \in Y\},$$

and their respective norms are (see [BKMT20], noting that the same norm characterization done there for Hilbert spaces holds also for the Banach case; see also [BL12])

$$\|r\|^2_{X\cap Y} = \|r\|^2_X + \|r\|^2_Y, \quad \|z\|^2_{X+Y} = \inf_{\substack{r=u+v,\\ u\in X, v\in Y}} \left[\|u\|^2_X + \|v\|^2_Y\right].$$

Furthermore, if $X \cap Y$ is dense in X and Y, then the following relation (understood as an identification under an isometry) holds

$$(X + Y)' = X' \cap Y'. \tag{1.1}$$

In addition, for a fixed positive constant α, by αX we denote the Banach space whose elements coincide with those in X but are measured with the norm $\|\bullet\|^2_{\alpha X} = \alpha^2 \|\bullet\|^2_X$.

Governing mathematical equations. Let $\Omega \subset \mathbb{R}^d$, with $d \in \{2,3\}$, be a simply connected, bounded, and Lipschitz domain occupied by a porous medium fully saturated with an incompressible fluid. Also, let $\Omega := \overline{\Gamma}_{\boldsymbol{u}} \cup \overline{\Gamma}_p$, and $\Gamma_{\boldsymbol{u}} \cap \Gamma_p = \phi$. Let $\boldsymbol{f} = (f_1,\ldots,f_d)^T$ be an external body force, and let g represent mass sources or sinks. The Darcy equations in mixed form involve determining the flux $\boldsymbol{u}$ and pressure p of the incompressible fluid, which must satisfy the following system of equations:

$$\kappa^{-1}\boldsymbol{u} - \nabla p = \boldsymbol{f} \quad \text{in } \Omega, \tag{1.2a}$$

$$\mathrm{div}\,\boldsymbol{u} = g \quad \text{in } \Omega, \tag{1.2b}$$

$$\boldsymbol{u}\cdot\boldsymbol{n} = 0 \quad \text{on } \Gamma_{\boldsymbol{u}}, \tag{1.2c}$$

$$p = 0 \quad \text{on } \Gamma_p, \tag{1.2d}$$

where $\kappa \in (0,1)$ represents the hydraulic conductivity, defined as the ratio of material permeability to fluid viscosity (instead of a constant positive κ, it can also be a positive defnite tensor), and $\boldsymbol{n}$ is the unit outward normal to the boundary $\partial\Omega$. The first equation suggests that fluid flow is governed by a pressure gradient, and the second equation ensures mass conservation.

Remark 1.1. *Let us remark here that $\kappa = 0$ physically represents the fact that the permeability of the fluid is zero, which means nothing but a static fluid, which is not of any physical significance. Another point worth mentioning is that, if the boundary conditions are pure Dirichlet or pure Neumann, then that changes the upcoming analysis as well while choosing the underlying spaces. See* [BKMT20] *for further details in this regard.*

Weak formulation of (1.2). We consider generic spaces $\mathbf{V}$ and Q for velocity and pressure, respectively (and to be made precise in the following). The weak formulation reads as follows: Find $(\boldsymbol{u}, p) \in \mathbf{V} \times \mathrm{Q}$ such that

$$a(\boldsymbol{u},\boldsymbol{v}) + b(\boldsymbol{v},p) = F(\boldsymbol{v}) \quad \forall \boldsymbol{v} \in \mathbf{V}, \tag{1.3a}$$

$$b(\boldsymbol{u}, q) = G(q) \quad \forall q \in \mathrm{Q}, \tag{1.3b}$$

where $\mathbf{V}$ (incorporating the flux boundary condition in an essential manner) and Q are sufficiently regular. The bilinear forms $a : \mathbf{V} \times \mathbf{V} \to \mathbb{R}$, $b : \mathbf{V} \times \mathrm{Q} \to \mathbb{R}$, linear functionals $F : \mathbf{V} \to \mathbb{R}$, $G : \mathrm{Q} \to \mathbb{R}$, respectively, are as follows

$$a(\boldsymbol{u}, \boldsymbol{v}) := \int_\Omega \kappa^{-1} \boldsymbol{u} \cdot \boldsymbol{v}, \quad b(\boldsymbol{v}, q) := \int_\Omega q \operatorname{div} \boldsymbol{v}, \quad F(\boldsymbol{v}) := \int_\Omega \boldsymbol{f} \cdot \boldsymbol{v}, \quad G(q) := \int_\Omega g\, q.$$

2. Continuous robust stability

We recall an abstract setting and its solvability using the Babuška–Brezzi framework, which we shall use it for the well-posedness of (1.3). A proof can be found in, e.g., [Gat14, Theorem 2.3].

Theorem 2.1 (Abstract setting)**.** *Let X, Y be two Hilbert spaces. Assume that $a(\bullet,\bullet)$ and $b(\bullet,\bullet)$ be two bounded bilinear forms, and*

$$Z := \{v \in X : b(v, q) = 0, \quad \forall q \in Y\}$$

be the kernel of $b(\bullet,\bullet)$, and assume that

- *(Z-ellipticity) the bilinear form $a(\bullet,\bullet)$ is Z-elliptic, that is, there exists a positive constant α such that*
$$a(u, u) \geq \alpha \|u\|_X^2 \qquad \forall u \in Z.$$
- *(Inf-sup condition) the bilinear form $b(\bullet,\bullet)$ satisfies the inf-sup condition, that is, there exists $\beta > 0$ such that*
$$\sup_{\substack{v \in X\\ v \neq 0}} \frac{b(v, q)}{\|v\|_X} \geq \beta \|q\|_Y \quad \forall q \in Y.$$

Then, for each $(f, g) \in X' \times Y'$ there exists a unique $(u, p) \in X \times Y$ such that

$$\begin{aligned} a(u, v) + b(v, p) &= f(v) \quad \forall v \in X,\\ b(v, q) &= g(q) \quad \forall q \in Y. \end{aligned}$$

Moreover, there exists $C > 0$, depending only on α, and β such that

$$\|(u, p)\|_{X \times Y} \leq C(\|f\|_{V'} + \|g\|_{Y'}). \tag{2.1}$$

For a robust well-posedness result, we now consider the following weighted spaces for velocity and pressure as follows

$$\mathbf{V} = \kappa^{-\frac{1}{2}} \mathbf{L}^2(\Omega) \cap \mathbf{H}_{\Gamma_{\boldsymbol{u}}}(\operatorname{div}, \Omega), \qquad \mathrm{Q} = \mathrm{L}^2(\Omega) + \kappa^{\frac{1}{2}} \mathrm{H}^1_{\Gamma_p}(\Omega), \tag{2.2}$$

endowed with the following norms;

$$\|\boldsymbol{v}\|_{\mathbf{V}} := \kappa^{-\frac{1}{2}} \|\boldsymbol{v}\|_{0,\Omega} + \|\operatorname{div} \boldsymbol{v}\|_{0,\Omega}, \tag{2.3a}$$

$$\|q\|_{\mathrm{Q}} := \inf_{\substack{q = q_1 + q_2,\\ (q_1, q_2) \in \mathrm{L}^2(\Omega) \times \mathrm{H}^1_{\Gamma_p}(\Omega)}} \left[\|q_1\|_{0,\Omega} + \kappa^{\frac{1}{2}} \|q_2\|_{1,\Omega}\right]. \tag{2.3b}$$

The following theorem proves the well-posedness of (1.3). Note that the majority of the idea remains the same as in [BKMT20], the differences occur only due to the change in the boundary conditions. For the sake of completeness, we provide the proof here. But before that, we prove the following lemma, which later assists in proving the continuous inf-sup condition.

Lemma 2.2. *There exists an operator $\mathcal{S}_c$ satisfying the following properties:*

$$\begin{gathered} \mathcal{S}_c \in \mathcal{L}(\mathrm{Q}', \mathbf{V}), \quad \|\mathcal{S}_c\|_{\mathcal{L}(\mathrm{Q}',\mathbf{V})} \text{ is independent of } \kappa, \quad \text{and}\\ \langle \operatorname{div}[\mathcal{S}_c(g)], \psi\rangle = \langle g, \psi\rangle \quad \text{for all } g \in \mathrm{Q}', \psi \in \mathrm{Q}, \end{gathered} \tag{2.4}$$

where $\beta_c = \left(\|\mathcal{S}_c\|_{\mathcal{L}(\mathrm{Q}',\mathbf{V})}\right)^{-1}$.

Proof. We proceed to define $\mathcal{S}_c$ as a bounded linear operator from two different spaces, and then, invoke the duality relation between sum and intersection between Banach spaces (1.1) to conclude that $\mathcal{S}_c \in \mathcal{L}(\mathrm{Q}', \mathbf{V})$.

Firstly, for the existence of $\mathcal{S} \in \mathcal{L}\big((\mathrm{H}^1_{\Gamma_p}(\Omega))', \mathbf{L}^2(\Omega)\big)$, let $\phi \in \mathrm{H}^1_{\Gamma_p}(\Omega)$ be the unique solution (thanks to [Gat14, Section 2.4.2]) of the following problem with mixed boundary conditions

$$-\Delta\phi = g \quad \text{on}\, \Omega, \quad \nabla\phi\cdot\boldsymbol{n} = 0 \quad \text{on}\, \Gamma_{\boldsymbol{u}}, \quad \phi = 0 \quad \text{on}\, \Gamma_p.$$

Then, defining $\mathcal{S}g := \nabla\phi$, it is straightforward that $\mathcal{S}_c \in \mathcal{L}\big((\mathrm{H}^1_{\Gamma_p}(\Omega))', \mathbf{L}^2(\Omega)\big)$. Note that, $\mathcal{S}_c$ satisfies all the three properties of (2.4).

Next, to show that $\mathcal{S}_c \in \mathcal{L}\left(\mathrm{L}^2(\Omega), \mathbf{H}_{\Gamma_{\boldsymbol{u}}}(\mathrm{div},\Omega)\right)$, consider $g \in \left(\mathrm{L}^2(\Omega)\right)'$. If $(\boldsymbol{w}, r) \in \mathbf{H}_{\Gamma_{\boldsymbol{u}}}(\mathrm{div},\Omega)\times\mathrm{L}^2(\Omega)$ be the unique solution of

$$\begin{aligned}(\boldsymbol{w},\boldsymbol{z}) + (\mathrm{div}\,\boldsymbol{z}, r) &= 0 \quad \forall \boldsymbol{z} \in \mathbf{H}_{\Gamma_{\boldsymbol{u}}}(\mathrm{div},\Omega),\\ (\mathrm{div}\,\boldsymbol{w}, s) &= \langle g, s\rangle \quad \forall s \in \mathrm{L}^2(\Omega).\end{aligned}$$

Then, defining $\mathcal{S}_c(g) := \boldsymbol{w}$, one obtains $\mathcal{S}_c \in \mathcal{L}\left(\mathrm{L}^2(\Omega), \mathbf{H}_{\Gamma_{\boldsymbol{u}}}(\mathrm{div},\Omega)\right)$. Note that, the above mixed problem is well-posed due to [BBF+13, Section 7.1.2].

Combining both the cases, and using the duality relation (1.1), we obtain

$$\mathcal{S}_c \in \mathcal{L}(\kappa^{\frac{1}{2}}(\mathrm{H}^1_{\Gamma_p}(\Omega))' \cap \mathrm{L}^2(\Omega), \kappa^{-\frac{1}{2}}\mathbf{L}^2(\Omega) \cap \mathbf{H}_{\Gamma_{\boldsymbol{u}}}(\mathrm{div},\Omega)) \implies \mathcal{S}_c \in \mathcal{L}\left(\mathrm{Q}', \mathbf{V}\right).$$

□

Let us now move forward with the continuous well-posedness of the weak form (1.3).

Theorem 2.3 (Robust stability)**.** *Consider the weighted spaces* (2.2)*, and assume that* $\mathbf{f} \in \mathbf{L}^2(\Omega), g \in \mathrm{L}^2(\Omega)$*. Then, there exists a unique* $(\boldsymbol{u}, p) \in \mathbf{V}\times\mathrm{Q}$ *solution to* (1.3)*. Furthermore, there exists a positive constant* $\tilde{C}$ *independent* κ*, such that*

$$\|(\boldsymbol{u},p)\|_{\mathbf{V}\times\mathrm{Q}} \le \tilde{C}(\|\boldsymbol{f}\|_{\mathbf{V}'} + \|g\|_{\mathrm{Q}'}). \tag{2.5}$$

Proof. We proceed to verify the assumptions of Theorem 2.1.

Continuity of $a(\bullet,\bullet)$ and $b(\bullet,\bullet)$. Let $\boldsymbol{u},\boldsymbol{v} \in \mathbf{V}$. Using the Cauchy-Schwarz inequality, one obtains the following

$$a(\boldsymbol{u},\boldsymbol{v}) = \kappa^{-1}(\boldsymbol{u},\boldsymbol{v}) \le \|\boldsymbol{u}\|_{\kappa^{-\frac{1}{2}}\mathbf{L}^2(\Omega)}\|\boldsymbol{v}\|_{\kappa^{-\frac{1}{2}}\mathbf{L}^2(\Omega)} \le \|\boldsymbol{u}\|_{\mathbf{V}}\|\boldsymbol{v}\|_{\mathbf{V}}.$$

To show the continuity of $b(\bullet,\bullet)$ we use a decomposition argument. Let $\mathrm{Q} \ni q = q_0 + q_1$, where $q_0 \in \mathrm{L}^2(\Omega)$ and $q_1 \in \mathrm{H}^1_{\Gamma_p}(\Omega)$. Then using integration-by-parts formula and the fact that $\boldsymbol{v} \in \mathbf{H}_{\Gamma_{\boldsymbol{u}}}(\mathrm{div},\Omega)$, and the Cauchy–Schwarz inequality, we deduce that

$$b(\boldsymbol{v},q) = (\mathrm{div}\,\boldsymbol{v}, q_0) - (\boldsymbol{v},\nabla q_1) \le \|\,\mathrm{div}\,\boldsymbol{v}\|_{\mathrm{L}^2(\Omega)}\|q_0\|_{\mathrm{L}^2(\Omega)} + \|\boldsymbol{v}\|_{\kappa^{-\frac{1}{2}}\mathbf{L}^2(\Omega)}\|\nabla q_1\|_{\kappa^{\frac{1}{2}}\mathbf{L}^2(\Omega)},$$

which upon using the identity $a_1a_2 + a_3a_4 \le (a_1^2 + a_3^2)^{\frac{1}{2}}(a_2^2 + a_4^2)^{\frac{1}{2}}$, with $a_1 = \kappa^{-\frac{1}{2}}\|\boldsymbol{v}\|_{\mathbf{L}^2(\Omega)}, a_2 = \|q_0\|_{\mathrm{L}^2(\Omega)}, a_3 = \|\,\mathrm{div}\,\boldsymbol{v}\|_{\mathrm{L}^2(\Omega)}, a_4 = \|\nabla q_1\|_{\kappa^{\frac{1}{2}}\mathbf{H}^1(\Omega)}$, gives the boundedness of $b(\bullet,\bullet)$ as follows.

$$b(\boldsymbol{v},q) \le \left(\kappa^{-1}\|\boldsymbol{v}\|^2_{\mathbf{L}^2(\Omega)} + \|\,\mathrm{div}\,\boldsymbol{v}\|^2_{\mathrm{L}^2(\Omega)}\right)^{\frac{1}{2}}\left(\|q_0\|^2_{\mathrm{L}^2(\Omega)} + \|\nabla q_1\|^2_{\kappa^{\frac{1}{2}}\mathbf{H}^1(\Omega)}\right)^{\frac{1}{2}} \le \|\boldsymbol{v}\|_{\mathbf{V}}\|q\|_{\mathrm{Q}}.$$

Note that, the last inequality is obtained by considering all such decompositions of $q = q_0 + q_1$ over Q.

$\mathbf{Z}$-ellipticity of $a(\bullet,\bullet)$. This follows immediately, as for all $\boldsymbol{v} \in \mathbf{Z}$,

$$a(\boldsymbol{v},\boldsymbol{v}) = \|\boldsymbol{v}\|^2_{\kappa^{-\frac{1}{2}}\mathbf{L}^2(\Omega)} = \|\boldsymbol{v}\|^2_{\mathbf{V}},$$

noting that the $\mathbf{H}(\mathrm{div})$-semi-norm is zero since $\boldsymbol{v} \in \mathbf{Z}$.

Inf-Sup condition for $b(\bullet,\bullet)$. This follows directly from Lemma 2.2, as demonstrated below.

$$\sup_{\boldsymbol{v}\in\mathbf{V}}\frac{(\operatorname{div}\boldsymbol{v},p)}{\|\boldsymbol{v}\|_{\mathbf{V}}}\geq\sup_{g\in\mathrm{Q}'}\frac{(\operatorname{div}\mathcal{S}g,p)}{\|\mathcal{S}g\|_{\mathbf{V}}}\geq\sup_{g\in\mathrm{Q}'}\frac{\langle g,p\rangle}{\|\mathcal{S}g\|_{\mathbf{V}}}\geq\frac{1}{\|\mathcal{S}\|_{\mathcal{L}(\mathrm{Q}',\mathbf{V})}}\sup_{g\in\mathrm{Q}'}\frac{\langle g,p\rangle}{\|g\|_{\mathrm{Q}'}}\geq\beta_c\|g\|_{\mathrm{Q}},\tag{2.6}$$

where $\beta_c:=\left(\|\mathcal{S}\|_{\mathcal{L}(\mathrm{Q}',\mathbf{V})}\right)^{-1}$.

It now remains to show the robust continuous dependence on the data. From the second equation of (1.3b), we arrive at

$$b(\boldsymbol{v},p)=\langle\boldsymbol{f},\boldsymbol{v}\rangle-a(\boldsymbol{u},\boldsymbol{v})\quad\forall\boldsymbol{v}\in\mathbf{V},$$

and then, a use of the continuous inf-sup stability (2.6) of $b(\bullet,\bullet)$, shows that

$$\beta_c\|p\|_{\mathrm{Q}}\leq\|\boldsymbol{f}\|_{\mathbf{V}'}+\|\boldsymbol{u}\|_{\mathbf{V}}.$$

Furthermore, since $\mathbf{Z}$ is a closed subspace of $\mathbf{V}$, $\boldsymbol{u}\in\mathbf{V}$ can be decomposed uniquely as $\boldsymbol{u}=\boldsymbol{u}^*+\widehat{\boldsymbol{u}}$, for $\boldsymbol{u}^*\in\mathbf{Z}$, and $\widehat{\boldsymbol{u}}\in\mathbf{Z}^\perp$. From (2.6), we note that (see for instance, [Gat14, Lemma 2.1])

$$\sup_{0\neq q\in\mathrm{Q}}\frac{b(\boldsymbol{v},q)}{\|q\|_{\mathrm{Q}}}\geq\beta_c\|\boldsymbol{v}\|_{\mathbf{V}}\quad\forall\boldsymbol{v}\in\mathbf{Z}^\perp.\tag{2.7}$$

Therefore, we now easily deduce from $b(\hat{\boldsymbol{u}},q)=\langle g,q\rangle$ that

$$\beta_c\|\hat{\boldsymbol{u}}\|_{\mathbf{V}}\leq\|g\|_{\mathrm{Q}'}.\tag{2.8}$$

Now, a use of the $\mathbf{Z}$-coercivity of $a(\bullet,\bullet)$ yields a bound on $\|\boldsymbol{u}^*\|_{\mathbf{V}}$ as given below

$$\|\boldsymbol{u}^*\|_{\mathbf{V}}\leq\|\boldsymbol{f}\|_{\mathbf{V}'}+\|\hat{\boldsymbol{u}}\|_{\mathbf{V}}\leq\|\boldsymbol{f}\|_{\mathbf{V}'}+\frac{1}{\beta_c}\|g\|_{\mathrm{Q}'}.\tag{2.9}$$

From (2.8), (2.9), and using the triangle inequality, we finally obtain an estimate for $\|\boldsymbol{u}\|_{\mathbf{V}}$ as follows.

$$\|\boldsymbol{u}\|_{\mathbf{V}}\leq\|\boldsymbol{u}^*\|_{\mathbf{V}}+\|\hat{\boldsymbol{u}}\|_{\mathbf{V}}\leq\|\boldsymbol{f}\|_{\mathbf{V}}+\frac{2}{\beta_c}\|g\|_{\mathrm{Q}}.\tag{2.10}$$

For an estimate on $\|p\|_{\mathrm{Q}}$, we simply use (2.7) and (2.10) to obtain

$$\|p\|_{\mathrm{Q}}\leq\frac{2}{\beta_c}\|\boldsymbol{f}\|_{\mathbf{V}'}+\frac{2}{\beta_c^2}\|g\|_{\mathrm{Q}'}.\tag{2.11}$$

This concludes the rest of the proof. □

3. Mixed finite element method

Let $\mathcal{T}_h$ be a regular simplicial mesh defined in a bounded Lipschitz domain Ω, consisting of tetrahedral elements (or triangular elements in two dimensions) K with diameter h_K. We define the mesh size as $h:=\max\{h_K:K\in\mathcal{T}_h\}$. Given an integer $k\geq0$ and a generic element $K\in\mathcal{T}_h$, we denote by $\mathbb{P}_k(K)$ the space of polynomials defined locally in K with a degree at most k, and denote by $\mathbb{P}_k(\mathcal{T}_h)$ its global counterpart

$$\mathbb{P}_k(\mathcal{T}_h):=\left\{p\in\mathrm{L}^2(\Omega):p|_K\in\mathbb{P}_k(K),\quad\forall K\in\mathcal{T}_h\right\}.$$

In addition, let $\mathbb{RT}_k(\mathcal{T}_h)$ denote the discrete $\mathbf{H}_{\Gamma_{\boldsymbol{u}}}(\operatorname{div},\Omega)$-conforming subspace defined by the Raviart–Thomas elements of order k, i.e.,

$$\mathbb{RT}_k(\mathcal{T}_h):=\{\boldsymbol{u}\in\mathbf{H}_{\Gamma_{\boldsymbol{u}}}(\operatorname{div},\Omega):\boldsymbol{u}|_K=[\mathbb{P}_k(K)]^d\oplus\widetilde{\mathbb{P}}_k(K)\boldsymbol{x},\ \boldsymbol{x}\in\Omega\subset\mathbb{R}^d,K\in\mathcal{T}_h\},$$

where we denote by $\widetilde{\mathbb{P}}_k(K)$ the space of all polynomials over K of degree exactly equal to k and $'\oplus'$ denotes the direct sum of spaces. With this we define the discrete weighted space for the velocity as all the vector fields in $\mathbb{RT}_k(\mathcal{T}_h)$ such that their $\mathbf{V}$ norm is bounded. Equivalently, and with the aim to emphasise the parameter-dependence, we write this space as

$$\mathbf{V}\supseteq\mathbf{V}_h:=\kappa^{-\frac{1}{2}}\mathbf{L}^2_h(\Omega)\cap\mathbf{H}_{h,\Gamma_{\boldsymbol{u}}}(\operatorname{div},\Omega),\tag{3.1}$$

where $\mathbf{L}^2_h(\Omega),\mathbf{H}_{h,\Gamma_{\boldsymbol{u}}}(\operatorname{div},\Omega)$ correspond to functions in $\mathbb{RT}_k(\mathcal{T}_h)$ equipped with the $\mathbf{L}^2(\Omega)$, and $\mathbf{H}(\operatorname{div},\Omega)$-norms, respectively.

In turn, define the discrete gradient operator $\nabla_h : \mathbb{P}_k(\mathcal{T}_h) \to \mathbb{RT}_k(\mathcal{T}_h)$ by (cf., [AFW97, eqn. (3.1)])

$$(\nabla_h q_h, \boldsymbol{v}_h) = -(\operatorname{div} \boldsymbol{v}_h, q_h), \quad \forall q_h \in \mathbb{P}_k(\mathcal{T}_h), \text{ and } \forall \boldsymbol{v}_h \in \mathbb{RT}_k(\mathcal{T}_h). \tag{3.2}$$

Next, we define the broken H^1-space as follows

$$\mathrm{H}^1(\mathcal{T}_h) := \{p \in \mathrm{L}^2(\Omega) : p|_K \in \mathrm{H}^1(K), \quad \forall K \in \mathcal{T}_h\},$$

and whenever needed we add a subscript Γ_i denoting the part on the boundary where the value of the function is prescribed to zero. These spaces are equipped with DG (broken Sobolev) seminorm

$$\mathrm{H}^1(\mathcal{T}_h) \ni \zeta \mapsto |\zeta|^2_{1,\mathcal{T}_h} := \left(\sum_{K \in \mathcal{T}_h} \|\nabla \zeta\|^2_{0,K} + \sum_{F \in \mathcal{F}_h} h_F^{-1} \|[\![\zeta]\!]\|^2_{0,F} \right)^{\frac{1}{2}},$$

where $\mathcal{F}_h$ denotes the set of facets in the mesh $\mathcal{T}_h$.

Furthermore, we define the following weighted space for pressure, which is a sum of the infinite-dimensional (but broken) spaces $\mathrm{L}^2(\Omega)$, $\mathrm{H}^1_{\Gamma_p}$:

$$\widehat{\mathrm{Q}}(\mathcal{T}_h) := \mathrm{L}^2(\Omega) + \kappa^{\frac{1}{2}} \mathrm{H}^1_{\Gamma_p}(\mathcal{T}_h). \tag{3.3}$$

In this space we define a broken weighted norm for any $q \in \widehat{\mathrm{Q}}(\mathcal{T}_h)$ as follows

$$\|q\|_{\widehat{\mathrm{Q}}(\mathcal{T}_h)} := \inf_{\substack{q = q_1 + q_2 \\ (q_1, q_2) \in \\ \mathrm{L}^2(\Omega) \times \mathrm{H}^1_{\Gamma_p}(\mathcal{T}_h)}} \left(\|q_1\|_{0,\Omega} + \kappa^{\frac{1}{2}} \, |q_2|_{1,\mathcal{T}_h} \right). \tag{3.4}$$

Finally, we define the discrete pressure space as all the functions in $\mathbb{P}_k(\mathcal{T}_h)$ whose $\widehat{\mathrm{Q}}_h(\mathcal{T}_h)$ norm is bounded

$$\mathrm{Q}_h := \kappa^{\frac{1}{2}} \mathrm{H}^1_{h,\Gamma_p}(\Omega) + \mathrm{L}^2_h(\Omega), \tag{3.5}$$

where $\mathrm{L}^2_h(\Omega), \mathrm{H}^1_h(\Omega)$ are polynomial spaces having discrete functions from $\mathbb{P}_k(\mathcal{T}_h)$, and equipped with the $\mathrm{L}^2(\Omega)$ norm and the broken $\mathrm{H}^1(\mathcal{T}_h)$ seminorm. The weighted mixed finite element formulation is to find $(\boldsymbol{u}_h, p_h) \in \mathbf{V}_h \times \mathrm{Q}_h$ satisfying

$$a(\boldsymbol{u}_h, \boldsymbol{v}_h) + b_h(\boldsymbol{v}_h, p_h) = \langle \boldsymbol{f}, \boldsymbol{v}_h \rangle \quad \forall \boldsymbol{v}_h \in \mathbf{V}_h, \tag{3.6a}$$

$$b_h(\boldsymbol{u}_h, q_h) = \langle g, q_h \rangle \quad \forall q_h \in \mathrm{Q}_h. \tag{3.6b}$$

Here,

$$a(\boldsymbol{u}_h, \boldsymbol{v}_h) = \int_\Omega \kappa^{-1} \boldsymbol{u}_h \cdot \boldsymbol{v}_h, \qquad b_h(\boldsymbol{v}_h, q_h) = \int_\Omega q_h \operatorname{div} \boldsymbol{v}_h.$$

Remark 3.1. *Let us remark here that since Q_h is not a subspace of Q, the discrete formulation entails a nonconforming scheme in the pressure term.*

Next, we prove the discrete counterpart of Lemma 2.2, which will be crucial to prove the discrete inf-sup constant.

Lemma 3.1. *There exists an operator $\mathcal{S}_d$ satisfying the following properties:*

$$\mathcal{S}_d \in \mathcal{L}(\mathrm{Q}_h', \mathbf{V}_h), \quad \|\mathcal{S}_d\|_{\mathcal{L}(\mathrm{Q}_h', \mathbf{V}_h)} \text{ is independent of } \kappa, h \quad \text{and}$$

$$\langle \operatorname{div}[\mathcal{S}_d(g_h)], \psi_h \rangle = \langle g_h, \psi_h \rangle \quad \text{for all } g_h \in \mathrm{Q}_h', \psi_h \in \mathrm{Q}_h. \tag{3.7}$$

Proof. We first define a bounded linear operator $\mathcal{S}_d$ from two different spaces, and then, invoke the duality relations between sum and intersection between Banach spaces (1.1) to conclude $\mathcal{S}_d \in \mathcal{L}(\mathrm{Q}_h', \mathbf{V}_h)$.

For the existence of $\mathcal{S}_d \in \mathcal{L}\big((\mathrm{H}^1_{h,\Gamma_p}(\Omega))', \mathbf{L}^2_h(\Omega)\big)$, let for a given $g_h \in (\mathrm{H}^1_{h,\Gamma_p}(\Omega))'$, $\phi_h \in \mathrm{H}^1_{h,\Gamma_p}(\Omega)$ be a unique solution to the following discrete problem

$$\langle \nabla_h \phi_h, \nabla_h \psi_h \rangle = \langle g_h, \psi_h \rangle \qquad \forall \psi_h \in \mathrm{H}^1_{h,\Gamma_p}(\Omega), \tag{3.8}$$

owing to the Banach–Nečas–Babuška theorem for elliptic problems in Banach spaces [EG21].

Then, it suffices to define $\mathcal{S}_d(g_h) := \nabla_h \phi_h$, where $\nabla_h \phi_h \in \mathbf{L}^2_h(\Omega)$. The continuous dependence on data coming from (3.8) also implies that $\|\mathcal{S}_d(g_h)\|_{0,\Omega} \lesssim \|g_h\|$. This, in turn, shows $\mathcal{S}_d \in \mathcal{L}\big((\mathrm{H}^1_{h,\Gamma_p}(\Omega))', \mathbf{L}^2_h(\Omega)\big)$.

Next, the existence and boundedness of $\mathcal{S}_d \in \mathcal{L}\big((\mathrm{L}^2_h(\Omega))', \mathbf{H}_{h,\Gamma_{\boldsymbol{u}}}(\mathrm{div},\Omega)\big)$ comes directly as a consequence of the surjectivity of the divergence operator from $\mathbf{H}_{\Gamma_{\boldsymbol{u}}}(\mathrm{div},\Omega)$ onto $\mathrm{L}^2(\Omega)$ and the standard properties of the Raviart–Thomas interpolation [BBF+13, Gat14]. $\square$

The following theorem is on robust well-posedness of the discrete weak formulation.

Theorem 3.2. *Consider the weighted spaces defined in* (3.1) *and* (3.5) *with the corresponding discrete weighted norms, and assume that* $\mathbf{f} \in \mathbf{L}^2(\Omega)$, $g \in \mathrm{L}^2(\Omega)$. *Then, there exists a unique* $(\boldsymbol{u}_h, p_h) \in \mathbf{V}_h \times \mathrm{Q}_h$ *solution to* (3.6). *Furthermore, there exists a positive constant* C *independent of* h, *and* κ, *such that*

$$\|(\boldsymbol{u}_h, p_h)\|_{\mathbf{V}_h \times \widehat{\mathrm{Q}}_h} \leq C\big(\|\boldsymbol{f}\|_{0,\Omega} + \|g\|_{0,\Omega}\big). \tag{3.9}$$

Proof. Note that the continuity of the bilinear forms and the coercivity of $a(\bullet,\bullet)$ on the kernel are similar to the continuous case. So, it is enough to prove the discrete inf-sup condition, which is again obtained straightforwardly by just using Lemma 3.1 as follows

$$\begin{aligned}
\sup_{\mathbf{0}\neq \boldsymbol{v}_h \in \mathbf{V}_h} \frac{|(\mathrm{div}\, \boldsymbol{v}_h, p_h)|}{\|\boldsymbol{v}_h\|_{\mathbf{V}}} &\geq \sup_{g_h \in \mathrm{Q}'_h} \frac{|(\mathrm{div}[\mathcal{S}_d(g_h)], p_h)|}{\|\mathcal{S}_d(g_h)\|_{\mathbf{V}}} = \sup_{g_h \in \mathrm{Q}'_h} \frac{|\langle g_h, p_h\rangle|}{\|\mathcal{S}_d(g_h)\|_{\mathbf{V}}} \\
&\geq \|\mathcal{S}_d\|^{-1}_{\mathcal{L}(\mathrm{Q}'_h, \mathbf{V}_h)} \sup_{g_h \in \mathrm{Q}'_h} \frac{|\langle g_h, p_h\rangle|}{\|g_h\|_{\mathrm{Q}'_h}} = \beta_d \|p_h\|_{\widehat{\mathrm{Q}}(\mathcal{T}_h)},
\end{aligned}$$

where $\beta_d := \|\mathcal{S}_d\|^{-1}_{\mathcal{L}(\mathrm{Q}'_h, \mathbf{V}_h)}$. This concludes the rest of the proof. $\square$

In this part, we state and prove an *a priori* estimate between the exact and discrete solutions of the Darcy equation, which is independent of κ and h. We recall, for a given subspace S_h of the generic Banach space $(S, \|\bullet\|_S)$, the notation $\mathrm{dist}(v, S_h) := \inf_{w \in S_h} \|v - w\|_S$.

Theorem 3.3 (Quasi-optimal error estimate)**.** *Let* $(\boldsymbol{u}, p)$ *and* $(\boldsymbol{u}_h, p_h)$ *uniquely solve the continuous model (1.3), and the discrete model (3.6), respectively. Then, there holds*

$$\|\boldsymbol{u} - \boldsymbol{u}_h\|_{\mathbf{V}} \leq 2\,\mathrm{dist}(\boldsymbol{u}, \mathbf{V}_h) + \frac{2}{\beta_d}\mathrm{dist}(p, \mathrm{Q}_h), \tag{3.10a}$$

$$\|p - p_h\|_{\widehat{\mathrm{Q}}(\mathcal{T}_h)} \leq \frac{2}{\beta_d}\,\mathrm{dist}(\boldsymbol{u}, \mathbf{V}_h) + \left(1 + \frac{2}{\beta_d^2}\right)\mathrm{dist}(p, \mathrm{Q}_h). \tag{3.10b}$$

Proof. Let $(\boldsymbol{u}_h^*, p_h^*) \in \mathbf{V}_h \times \mathrm{Q}_h$ be an arbitrary element. For $(\boldsymbol{v}_h, q_h) \in \mathbf{V}_h \times \mathrm{Q}_h$, let us subtract (3.6) from (1.3), and using the arbitrary element $(\boldsymbol{u}_h^*, p_h^*)$, we obtain

$$a\left(\boldsymbol{u}_h - \boldsymbol{u}_h^*, \boldsymbol{v}_h\right) + b_h\left(\boldsymbol{v}_h, p_h - p_h^*\right) = a\left(\boldsymbol{u} - \boldsymbol{u}_h^*, \boldsymbol{v}_h\right) + b_h\left(\boldsymbol{v}_h, p - p_h^*\right), \tag{3.11}$$

$$b_h\left(\boldsymbol{u}_h - \boldsymbol{u}_h^*, q_h\right) = b_h\left(\boldsymbol{u} - \boldsymbol{u}_h^*, q_h\right). \tag{3.12}$$

Since $(\boldsymbol{u}_h - \boldsymbol{u}_h^*) \in \mathbf{V}_h$, and $(p_h - p_h^*) \in \mathrm{Q}_h$, an appeal to the discrete robust stability estimates in Theorem 3.2 implies

$$\begin{aligned}
\|\boldsymbol{u}_h - \boldsymbol{u}_h^*\|_{\mathbf{V}} &\leq \|\boldsymbol{u} - \boldsymbol{u}_h^*\|_{\mathbf{V}} + \frac{2}{\beta_d}\|p - p_h^*\|_{\widehat{\mathrm{Q}}(\mathcal{T}_h)}, \\
\|p_h - p_h^*\|_{\mathrm{Q}_h} &\leq \frac{2}{\beta_d}\|\boldsymbol{u} - \boldsymbol{u}_h^*\|_{\mathbf{V}} + \frac{2}{\beta_d^2}\|p - p_h^*\|_{\widehat{\mathrm{Q}}(\mathcal{T}_h)}.
\end{aligned}$$

Next, we use the triangle inequality to derive the following error estimates for the flux and pressure.

$$\begin{aligned}
\|\boldsymbol{u} - \boldsymbol{u}_h\|_{\mathbf{V}} &\leq 2\,\mathrm{dist}(\boldsymbol{u}, \mathbf{V}_h) + \frac{2}{\beta_d}\mathrm{dist}(p, \mathrm{Q}_h), \\
\|p - p_h\|_{\widehat{\mathrm{Q}}(\mathcal{T}_h)} &\leq \frac{2}{\beta_d}\,\mathrm{dist}(\boldsymbol{u}, \mathbf{V}_h) + \left(1 + \frac{2}{\beta_d^2}\right)\mathrm{dist}(p, \mathrm{Q}_h).
\end{aligned}$$

$\square$

Note that $\mathbf{Z}_h \subset \mathbf{Z}$ produces a robust pressure estimate for the velocity.

Corollary 3.3.1. *Under the assumptions of Theorem 3.3, there is*

$$\|\boldsymbol{u} - \boldsymbol{u}_h\|_{\mathbf{V}} \leq C_D \operatorname{dist}(\boldsymbol{u}, \boldsymbol{v}_h),$$

where C_D is independent of h and κ.

Proof. The proof proceeds by selecting $\boldsymbol{u}_h^g \in \mathbf{Z}_h$ and noting that $\boldsymbol{u}_h - \boldsymbol{u}_h^g \in \mathbf{Z}_h$. By the $\mathbf{Z}$-coercivity of the bilinear form $a(\cdot,\cdot)$, together with the identity

$$a(\boldsymbol{u}_h^g - \boldsymbol{u}_h, \boldsymbol{v}_h) = a(\boldsymbol{u} - \boldsymbol{u}_h^g, \boldsymbol{v}_h), \quad \forall \boldsymbol{v}_h \in \mathbf{Z}_h,$$

and choosing $\boldsymbol{v}_h = \boldsymbol{u}_h^g - \boldsymbol{u}_h$, we obtain the desired estimate. □

Next, in order to provide a theoretical convergence rate for mixed FEM (1.3), we recall the approximation properties of the subspaces involved.

Let $t \in (1,\infty)$ and denote by $\Pi_h : \mathbf{W}^{l,t}(\Omega) \cap \mathbf{H}(\operatorname{div}_{1,t},\Omega) \to \mathbb{RT}_k(\mathcal{T}_h)$ the Fortin operator and by $P_h : \mathrm{W}^{l,t}(K) \to \mathbb{P}_k(K)$, the local orthogonal L^2 projection. Then, as a standard consequence of the Bramble–Hilbert lemma, optimal approximation, and inverse inequalities on polynomial spaces, we can assert that

$$\|\boldsymbol{v} - \Pi_h \boldsymbol{v}\|_{m,t,\Omega} \leq C_1 h^{l-m} |\boldsymbol{v}|_{l,t,\Omega} \quad \forall \boldsymbol{v} \in \mathbf{W}^{l,t}(\Omega),\ 1 \leq l \leq k+1, \tag{3.14a}$$

$$\|\operatorname{div}(\boldsymbol{v} - \Pi_h \boldsymbol{v})\|_{m,t,\Omega} \leq C_2 h^{l-m} |\operatorname{div} \boldsymbol{v}|_{l,t,\Omega} \quad \forall \boldsymbol{v} \in \mathbf{W}^{1,t}(\Omega),\ \text{with}\ \operatorname{div}(\boldsymbol{v}) \in \mathrm{W}^{1,t}(\Omega)\ \text{and}\ 0 \leq l \leq k+1, \tag{3.14b}$$

$$\|q - P_h q\|_{m,t,\Omega} \leq C_2 h^{l-m} |p|_{l,t,\Omega} \quad \forall q \in \mathrm{W}^{l,t}(\Omega),\ 0 \leq l \leq k+1, \tag{3.14c}$$

$$\|\nabla(q - P_h q)\|_{0,t,K} \leq C_3 h_K^l |p|_{l+1,t,K} \quad \forall q \in \mathrm{W}^{l+1,t}(K),\ K \in \mathcal{T}_h,\ l \leq k, \tag{3.14d}$$

for $0 \leq m \leq l$, where $C_1, C_2 > 0$ are independent of h and $C_3 > 0$ is independent of h_K (see [GMRB22, Sections 4.1 and 4.5] for the first three, and [EG21] for the fourth one).

To conclude this section, the following theorem provides the theoretical rate of convergence for (1.3), under suitable regularity assumptions on the exact solution.

Theorem 3.4 (Convergence rates)**.** *Let $(\boldsymbol{u}, p) \in \mathbf{V} \times \mathrm{Q}$ be the solution of the continuous problem (1.2) with the following additional conditions of regularity:*

$$\boldsymbol{u} \in \kappa^{-\frac{1}{2}} \mathbf{H}^l(\Omega), \quad \operatorname{div} \boldsymbol{u} \in \mathrm{H}^l(\Omega), \quad \text{and} \quad p = p_1 + p_2,$$
$$\text{with} \quad p_1 \in \mathrm{H}^l(\Omega), \quad p_2 \in \kappa^{\frac{1}{2}} \mathrm{H}^{l+1}(\Omega),$$

where $1 \leq l \leq k+1$. Then, there exist positive constants $C_\sharp, C_\flat > 0$, independent of h, κ, such that

$$\|\boldsymbol{u} - \boldsymbol{u}_h\|_{\mathbf{V}} + \|p - p_h\|_{\widehat{\mathrm{Q}}(\mathcal{T}_h)} \leq C_\sharp h^l \big[\kappa^{-\frac{1}{2}} \|\boldsymbol{u}\|_{l,\Omega} + \|\operatorname{div} \boldsymbol{u}\|_{l,\Omega} + C_\flat h^l \big[|p_1|_{l,\Omega} + \kappa^{\frac{1}{2}} |p_2|_{l+1,\Omega}\big].$$

Proof. We first take $m = 0$ in (3.14a), which leads to

$$\|\boldsymbol{u} - \Pi_h \boldsymbol{u}\|_{0,\Omega} \leq C_1 h^l |\boldsymbol{u}|_{l,\Omega}.$$

We also take $m = 0$ and $t = 2$ in (3.14b), which gives

$$\|\operatorname{div}(\boldsymbol{u} - \Pi_h \boldsymbol{u})\|_{0,\Omega} \leq C_2 h^l |\boldsymbol{u}|_{l,\Omega},$$

select $1 \leq l \leq k+1$ for the last two estimates displayed. Therefore, owing to Corollary 3.3.1, we arrive at the velocity error bound

$$\|\boldsymbol{u} - \boldsymbol{u}_h\|_{\mathbf{V}} \leq C_D \operatorname{dist}(\boldsymbol{u}, \mathbf{V}_h) \leq C_D C_1 C_2 h^l (\kappa^{-\frac{1}{2}} \|\boldsymbol{u}\|_{l,\Omega} + \|\operatorname{div} \boldsymbol{u}\|_{l,\Omega}).$$

For pressure we decompose $p = p_1 + p_2$, employ the properties of the sum norm (3.4), apply (3.14c) to $m = 0$ and $t = 2$, and (3.14d) to $t = 2$, summed over $K \in \mathcal{T}_h$. We combine that with the following trace inequality to control the jump term in the broken norms

$$h_F^{1-t} \|[\![p_j - P_h p_j]\!]\|_{0,t,F}^t = h_F^{1-t} \|[\![P_h p_j]\!]\|_{0,t,F}^t \leq C_3 h^{lt} |p_j|_{l+1,r,\omega_F}^t,$$

where ω_F stands for the usual patch on the face. We apply this for $j = 2$ with $t = 2$, and we readily obtain

$$\begin{aligned}\|p - P_h p\|_{\widehat{\mathrm{Q}}(\mathcal{T}_h)} &\le \|p_1 - P_h p_1\|_{0,\Omega} + \kappa^{\frac{1}{2}} |p_2 - P_h p_2|_{1,\mathcal{T}_h} \\ &\le \max\{C_2, C_3\} h^l \big(|p_1|_{l,\Omega} + \kappa^{\frac{1}{2}} |p_2|_{l+1,\Omega}\big).\end{aligned}$$

Then we can directly invoke the quasi-optimality estimate from Theorem 3.3, to get the desired result with $C_\sharp = C_D(2C_1 + C_2)$ and $C_\flat = \widetilde{C}_g \max\{C_2, C_3\}$. Since the last two contributions of the pressure norm require derivatives, the projection L^2 only delivers theoretical approximability if $k \ge 1$ or if the infimum decomposition can be chosen such that $p = p_1$ (and $p_2 = 0$), i.e., if the optimal decomposition lives entirely in the component L^2. □

4. Numerical Results

The purpose of this section is to experimentally validate the theoretical results presented in the previous section. We verify that the convergence rates are robust in the proposed finite element method and also illustrate the performance of proposed schemes in typical porous media flow problems. The numerical implementation is based on the open-source finite element framework `Gridap` [BMV22], and the main routines can be publicly accessed from https://github.com/rishidas-04/GridapRobustDarcy.

Example 1a (convergence test against smooth solutions in 2D). Consider the unit square domain $\Omega = (0,1)^2$ along with the following manufactured solutions

$$p(x,y) = \sin(\pi x)\cos(\pi y), \qquad \text{and } \boldsymbol{u}(x,y) := \begin{pmatrix} \cos(\pi x)\sin(\pi y) \\ -\sin(\pi x)\cos(\pi y)\end{pmatrix}.$$

We set the left and bottom sides of the square as $\Gamma_{\boldsymbol{u}}$ and the top and right sides as Γ_p. The forcing vector and the fluid source g, as well as the essential boundary condition (non-homogeneous) in the flux, are calculated based on the manufactured solutions above. We take a simple dimensional unity parameter $\kappa = 1$. The error history associated with the proposed mixed finite element method on a sequence of successively refined partitions of the domain is presented in Table 5.1, where we also tabulate the error decay rates calculated as $\texttt{rate} = \log(e_{(\bullet)}/\tilde{e}_{(\bullet)})[\log(h/\tilde{h})]^{-1}$, where $e, \tilde{e}$ denote errors generated on two consecutive meshes of sizes h and $\tilde{h}$, respectively. The results indicate optimal convergence in all fields and for the two tested polynomial degrees. Moreover, a maximum of four iterations is required by the Newton–Raphson method to reach a tolerance (absolute or relative) of 10^{-8} on the residual. The approximate solutions of the samples for velocity and pressure obtained with the second-order method (with $k = 1$) are plotted in Figure

Example 1b (convergence test against smooth solutions in 3D). Consider the unit cube domain $\Omega = (0,1)^3$ along with the following smooth manufactured solutions

$$p(x,y,z) := \sin(\pi x)\cos(\pi y)\sin(\pi z), \quad \boldsymbol{u}(x,y,z) := \begin{pmatrix} \cos(\pi x)\sin(\pi y)\sin(\pi z) \\ -\sin(\pi x)\cos(\pi y)\sin(\pi z) \\ \sin(\pi x)\sin(\pi y)\cos(\pi z)\end{pmatrix}.$$

We set the left, bottom, and front sides of the cube as $\Gamma_{\boldsymbol{u}}$ and the right, top, and back sides as Γ_p. The forcing vector and the fluid source g, as well as the essential boundary condition (non-homogeneous) in the flux, are calculated based on the manufactured solutions above. We take, for this first set of examples, simply dimensional unity parameters $\kappa = 1$. The error history associated with the proposed mixed finite element method in a sequence of successively refined partitions of the domain is presented in Table 5.2, where we also tabulate the decay rates of errors calculated as $\texttt{rate} = \log(e_{(\bullet)}/\tilde{e}_{(\bullet)})[\log(h/\tilde{h})]^{-1}$, where $e, \tilde{e}$ denote the errors generated on two consecutive meshes of sizes h and $\tilde{h}$, respectively. The results indicate optimal convergence in all fields and for the two tested polynomial degrees. Moreover, for this problem the number of Newton-Raphson iterations required to reach a tolerance (either absolute or relative) of 10^{-8} is up to seven. This depends on the initial guess, and here we have used a constant velocity and pressure such that every entry of the vector of degrees of freedom is 10^{-4}. Sample approximate solutions for velocity and pressure obtained with the second-order method (with $k = 1$) are plotted in Figure. For

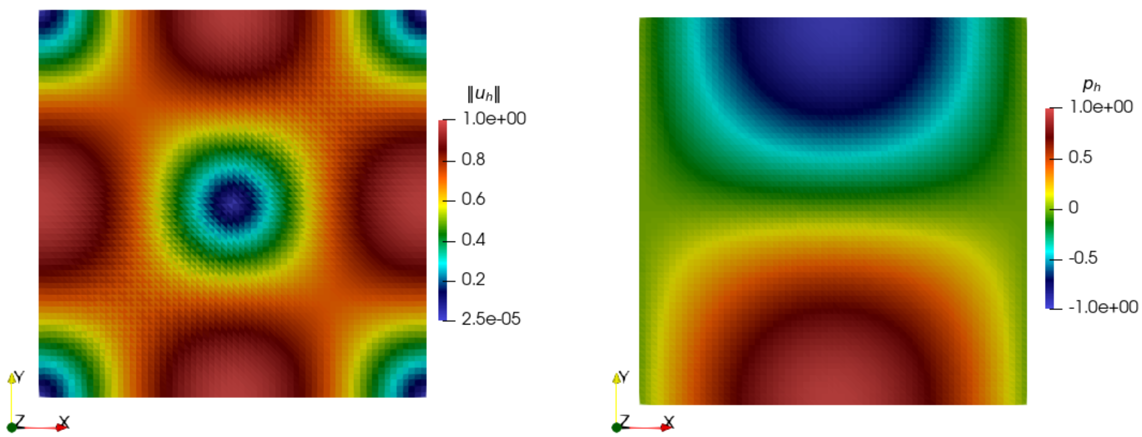

FIGURE 4.1. Example 1a. approximate velocity (left) and pressure (right) for the accuracy test of the Darcy equations with unit parameters.

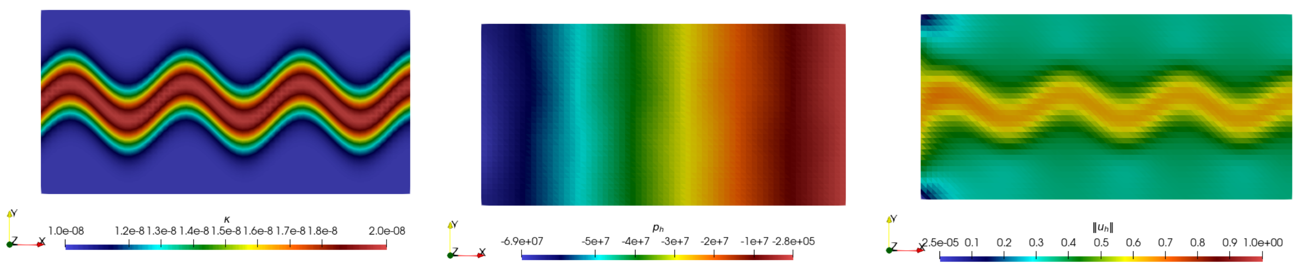

FIGURE 4.2. Example 2. Sample of heterogeneous permeability, pressure profile, and filtration velocity magnitude for the convergence test with reference solutions.

these results, we consider the norms $\mathbf{H}(\mathrm{div},\Omega)$ and $\mathrm{L}^2(\Omega)$ for velocity and pressure (with no parameter weighting).

Example 2 (Experimental self-convergence). For a second run of simulations we use the domain $\Omega = (0,2)\times(0,1)$ without a known analytical solution, setting the problem data as $= \mathbf{0}$, $g = 0$, mixed boundary conditions as follows $\boldsymbol{u}\cdot\boldsymbol{n} = 2.5y(1-y)$ on the left segment, $\boldsymbol{u}\cdot\boldsymbol{n} = 0$ on the top and bottom segments, and $p = 0$ on the right edge. The permeability is heterogeneous $\kappa(\boldsymbol{x}) = \kappa_0(1+\exp(-\frac{1}{2}[10y-5-\sin(10x)]^2)$, and we consider the more pronounced parameter values $\kappa_0 = 10^{-8}$. In Table 5.3, we show the error decay where we compute experimental errors against a fine-mesh reference solution $\boldsymbol{u}_{\mathrm{ref}}, p_{\mathrm{ref}}$(with two more refinement steps than the finest level). In the first part of the table we use the non-weighted norms and we see very large errors in the pressure and a sub-optimal error decay for the velocity in the second-order case. In contrast, for the second part of the table, errors are now measured in the weighted norms associated with $\mathbf{V}$ and $\widehat{\mathrm{Q}}(\mathcal{T}_h)$ respectively, where we move the scaling of the now variable permeability within the norm definition. We recall from [BKMT20] that in the space Q_h the realization of the discrete weighted Laplacian operator required that is the Riesz map for $\kappa^{\frac{1}{2}}\mathrm{H}^1_{h,\Gamma_p}(\Omega)$ is as follows

$$\langle -\operatorname{div}(\kappa(\boldsymbol{x})\nabla p_h), q_h\rangle = \sum_{K\in\mathcal{T}_h}(\kappa(\boldsymbol{x})\nabla p_h, \nabla q_h)_K + \sum_{F\in\mathcal{E}_h\cup\mathcal{E}_h^{\Gamma_p}}\frac{1}{h_F}(\kappa(\boldsymbol{x})[\![p_h]\!], [\![q_h]\!])_F.$$

Here $\mathcal{E}_h$ denotes the set of internal facets, $\mathcal{E}_h^{\Gamma_p}$ denotes the set of facets lying on the sub-boundary Γ_p, and $[\![\bullet]\!]$ represents the jump operator across a facet (and adopt the convention that it reduces to the identity if the face lies on the boundary).

DoF	h	$\|u-u_h\|_{\mathrm{div},\Omega}$	rate	$\|p-p_h\|_{0,\Omega}$	rate	$\|P_h(\mathrm{div}(\boldsymbol{u}_h)-g)\|_{\mathrm{L}^\infty}$
Errors and convergence rates for $k=0$						
20	0.7071	4.76e-01	$\star$	2.43e-01	$\star$	4.08e-16
80	0.3536	2.64e-01	0.848	1.29e-01	0.920	2.62e-15
320	0.1768	1.37e-01	0.949	6.52e-02	0.980	4.26e-14
1280	0.0884	6.92e-02	0.985	3.27e-02	0.995	9.02e-12
5120	0.0442	3.47e-02	0.996	1.64e-02	0.999	7.79e-11
20480	0.0221	1.74e-02	0.999	8.18e-03	1.000	3.62e-09
Errors and convergence rates for $k=1$						
64	0.7071	1.48e-01	$\star$	7.34e-02	$\star$	2.88e-14
256	0.3536	4.06e-02	1.861	1.95e-02	1.911	1.80e-13
1024	0.1768	1.05e-02	1.947	4.95e-03	1.978	1.82e-12
4096	0.0884	2.67e-03	1.982	1.24e-03	1.995	1.76e-10
16384	0.0442	6.70e-04	1.994	3.11e-04	1.999	7.13e-10
65536	0.0221	1.68e-04	1.998	7.78e-05	2.000	1.08e-08

DoF	h	$\|u-u_h\|_{\mathbf{V}}$	rate	$\|p-p_h\|_{\widehat{\mathrm{Q}}(\mathcal{T}_h)}$	rate	$\|P_h(\mathrm{div}(\boldsymbol{u}_h)-g)\|_{\mathrm{L}^\infty}$
Errors and convergence rates for $k=0$						
20	0.7071	4.76e-01	$\star$	6.33e-02	$\star$	4.08e-16
80	0.3536	2.64e-01	0.848	1.71e-02	1.886	2.62e-15
320	0.1768	1.37e-01	0.949	4.35e-03	1.980	4.26e-14
1280	0.0884	6.92e-02	0.985	1.09e-03	1.994	9.02e-12
5120	0.0442	3.47e-02	0.996	2.73e-04	1.997	7.79e-11
20480	0.0221	1.74e-02	0.999	6.84e-05	1.999	3.62e-09
Errors and convergence rates for $k=1$						
64	0.7071	1.48e-01	$\star$	1.82e-01	$\star$	2.88e-14
256	0.3536	4.06e-02	1.861	5.42e-02	1.752	1.80e-13
1024	0.1768	1.05e-02	1.947	1.41e-02	1.938	1.82e-12
4096	0.0884	2.67e-03	1.982	3.58e-03	1.983	1.76e-10
16384	0.0442	6.70e-04	1.994	8.97e-04	1.995	7.13e-10
65536	0.0221	1.68e-04	1.998	2.24e-04	1.999	1.08e-08

TABLE 4.1. Example 1a : Error history for velocity and pressure with respect to the usual $\mathbf{H}(\mathrm{div},\Omega)$-$\mathrm{L}^2(\Omega$ (top rows) and the parameter-weighted norms (bottom rows) in 2D for unit parameter $\kappa = 1$.

Example 3a (operator preconditioning). The following preconditioners have been discussed in [BKMT20].

$$\mathcal{B}_1 := \begin{pmatrix} (\kappa^{-1}\mathcal{I} - \kappa^{-1}\nabla\,\mathrm{div})^{-1} & 0 \\ 0 & \kappa\mathcal{I}^{-1} \end{pmatrix}, \tag{4.1}$$

and

$$\mathcal{B}_2 := \begin{pmatrix} (\kappa^{-1}\mathcal{I} - \nabla\,\mathrm{div})^{-1} & 0 \\ 0 & \mathcal{I}^{-1} + (-\kappa\Delta)^{-1} \end{pmatrix}. \tag{4.2}$$

We perform a series of computations in which the permeability κ is varied by several orders of magnitude. This is done again using the domain $\Omega = (0,1)^2$, the lowest-order finite element family, and mixed boundary conditions as in Example 1a. The performance of the numerical method is assessed by comparing an estimate of the condition number of the preconditioned system matrix with the preconditioners mentioned above, and also inspecting the number of MinRes iterations required to solve the preconditioned system. Table 4.4 illustrates the robustness of the proposed preconditioner across the parametric space. Additionally, the performance of the preconditioner corresponding to the weighted Riesz map (4.1) has also been illustrated in Table 4.4, which seems to perform slightly better than (4.2). This is a behaviour

DoF	h	$\|u-u_h\|_{\mathrm{div},\Omega}$	rate	$\|p-p_h\|_{0,\Omega}$	rate	$\|P_h(\mathrm{div}(\boldsymbol{u}_h)-g)\|_{\mathrm{L}^\infty}$
Errors and convergence rates for $k=0$						
144	0.7071	9.42e-01	$\star$	1.79e-01	$\star$	1.04e-14
1152	0.3536	5.07e-01	0.892	9.59e-02	0.902	7.09e-12
9216	0.1768	2.59e-01	0.968	4.88e-02	0.975	2.18e-09
73728	0.0884	1.30e-01	0.992	2.45e-02	0.994	6.85e-09
Errors and convergence rates for $k=1$						
624	0.7071	3.32e-01	$\star$	6.29e-02	$\star$	2.35e-13
4992	0.3536	9.17e-02	1.855	1.73e-02	1.867	3.43e-12
39936	0.1768	2.36e-02	1.958	4.42e-03	1.966	2.43e-09
319488	0.0884	5.95e-03	1.988	1.11e-03	1.992	1.06e-07

Table 4.2. Example 1b : Error history for velocity and pressure with respect to the usual $\mathbf{H}(\mathrm{div},\Omega)$-$\mathrm{L}^2(\Omega$ in 3D for unit parameter $\kappa=1$.

very similar to the one reported in [BKMT20], but the map (4.1) is preferable in a multiphysics context where the scaling of the divergence component of the velocity block is not feasible.

References

[AFW97] Douglas Arnold, Richard Falk, and Ragnar Winther, *Preconditioning in h (div) and applications*, Mathematics of computation **66** (1997), no. 219, 957–984.

[BBF+13] Daniele Boffi, Franco Brezzi, Michel Fortin, et al., *Mixed finite element methods and applications*, vol. 44, Springer, 2013.

[BKMRB21] Wietse M Boon, Miroslav Kuchta, Kent-Andre Mardal, and Ricardo Ruiz-Baier, *Robust preconditioners for perturbed saddle-point problems and conservative discretizations of biot's equations utilizing total pressure*, SIAM Journal on Scientific Computing **43** (2021), no. 4, B961–B983.

[BKMT20] Trygve Bærland, Miroslav Kuchta, Kent-Andre Mardal, and Travis Thompson, *An observation on the uniform preconditioners for the mixed darcy problem*, Numerical Methods for Partial Differential Equations **36** (2020), no. 6, 1718–1734.

[BL12] Jöran Bergh and Jörgen Löfström, *Interpolation spaces: an introduction*, Springer Science & Business Media, 2012.

[BMV22] Santiago Badia, Alberto F Martín, and Francesc Verdugo, *Gridapdistributed: a massively parallel finite element toolbox in julia*, Journal of Open Source Software **7** (2022), no. 74, 4157.

[BV20] Santiago Badia and Francesc Verdugo, *Gridap: an extensible finite element toolbox in julia*, Journal of Open Source Software **5** (2020), no. 52, 2520.

[DHPRB26] Rishi Das, Harsha Hutridurga, Amiya K. Pani, and Ricardo Ruiz-Baier, *Robust stability and preconditioning of Darcy–Forchheimer equations*, SIAM Journal on Numerical Analysis (2026), (Accepted).

[EG21] Alexandre Ern and Jean-Luc Guermond, *Finite elements i: Approximation and interpolation*, vol. 72, Springer Nature, 2021.

[Gat14] Gabriel N Gatica, *A simple introduction to the mixed finite element method*, Theory and Applications. Springer Briefs in Mathematics. Springer, London (2014).

[GMRB22] Gabriel N Gatica, Salim Meddahi, and Ricardo Ruiz-Baier, *An l p spaces-based formulation yielding a new fully mixed finite element method for the coupled darcy and heat equations*, IMA Journal of Numerical Analysis **42** (2022), no. 4, 3154–3206.

[GOS11] Gabriel Gatica, Ricardo Oyarzúa, and Francisco-Javier Sayas, *Analysis of fully-mixed finite element methods for the stokes-darcy coupled problem*, Mathematics of Computation **80** (2011), no. 276, 1911–1948.

[HKK+22] Qingguo Hong, Johannes Kraus, Miroslav Kuchta, Maria Lymbery, Kent-André Mardal, and Marie E Rognes, *Robust approximation of generalized biot-brinkman problems*, Journal of Scientific Computing **93** (2022), no. 3, 77.

[Kir10] Robert C Kirby, *From functional analysis to iterative methods*, SIAM review **52** (2010), no. 2, 269–293.

[MW11] Kent-Andre Mardal and Ragnar Winther, *Preconditioning discretizations of systems of partial differential equations*, Numerical Linear Algebra with Applications **18** (2011), no. 1, 1–40.

[OS20] D Orban and AS Siqueira, *contributors. linearoperators. jl*, 2020.

DoF	h	$\|u - u_h\|_{\mathrm{div},\Omega}$	rate	$\|p - p_h\|_{0,\Omega}$	rate	$\|P_h(\mathrm{div}(\boldsymbol{u}_h) - g)\|_{\mathrm{L}^\infty}$
Errors and convergence rates for $k = 0$						
36	0.7071	5.28e-01	$\star$	1.02e+07	$\star$	6.66e-16
84	0.3536	4.26e-01	0.309	3.86e+06	1.403	2.54e-15
240	0.1768	4.53e-01	-0.088	1.78e+06	1.122	1.05e-14
792	0.0884	2.75e-01	0.718	6.29e+05	1.497	1.30e-12
2856	0.0442	1.52e-01	0.855	1.93e+05	1.707	6.71e-11
10824	0.0221	8.26e-02	0.881	6.53e+04	1.561	2.88e-10
Errors and convergence rates for $k = 1$						
120	0.7071	3.81e-01	$\star$	1.17e+06	$\star$	3.06e-14
276	0.3536	3.62e-01	0.072	6.21e+05	0.915	1.21e-13
780	0.1768	2.43e-01	0.574	2.28e+05	1.443	1.69e-12
2556	0.0884	1.11e-01	1.132	7.72e+04	1.565	2.07e-12
9180	0.0442	3.73e-02	1.574	2.34e+04	1.724	1.76e-10
34716	0.0221	1.25e-02	1.579	6.37e+03	1.876	1.01e-09

DoF	h	$\|u - u_h\|_{\mathbf{V}}$	rate	$\|p - p_h\|_{\widehat{\mathrm{Q}}(\mathcal{T}_h)}$	rate	$\|P_h(\mathrm{div}(\boldsymbol{u}_h) - g)\|_{\mathrm{L}^\infty}$
Errors and convergence rates for $k = 0$						
36	0.7071	1.44e+03	$\star$	7.19e+02	$\star$	6.66e-16
84	0.3536	5.93e+02	1.275	2.65e+02	1.438	2.54e-15
240	0.1768	3.64e+02	0.705	1.14e+02	1.213	1.05e-14
792	0.0884	1.64e+02	1.153	4.08e+01	1.489	1.30e-12
2856	0.0442	5.24e+01	1.643	1.24e+01	1.718	6.71e-11
10824	0.0221	2.17e+01	1.272	3.17e+00	1.969	2.88e-10
Errors and convergence rates for $k = 1$						
120	0.7071	4.80e+02	$\star$	1.67e+02	$\star$	3.06e-14
276	0.3536	2.23e+02	1.104	3.65e+01	2.199	1.21e-13
780	0.1768	1.10e+02	1.022	1.29e+01	1.504	1.69e-12
2556	0.0884	3.39e+01	1.699	5.59e+00	1.200	2.07e-12
9180	0.0442	6.98e+00	2.280	2.56e+00	1.129	1.76e-10
34716	0.0221	1.16e+00	2.593	6.80e-01	1.912	1.01e-09

TABLE 4.3. Example 2 : Error history for velocity and pressure with respect to the usual parameter-independent norms (top rows) and weighted norms (bottom rows) with $\kappa = 10^{-8}$.

IITB-MONASH RESEARCH ACADEMY, INDIAN INSTITUTE OF TECHNOLOGY BOMBAY, POWAI, MUMBAI 400076, MAHARASHTRA, INDIA

Email address: rishi.das@monash.edu

DEPARTMENT OF MATHEMATICS, INDIAN INSTITUTE OF TECHNOLOGY BOMBAY, POWAI, MUMBAI 400076, MAHARASHTRA, INDIA

Email address: hutridurga@iitb.ac.in

DEPARTMENT OF MATHEMATICS, BITS PILANI, K. K. BIRLA GOA CAMPUS, ZUARINAGAR, GOA 403726, INDIA

Email address: amiyap@goa.bits-pilani.ac.in

SCHOOL OF MATHEMATICS, MONASH UNIVERSITY, 9 RAINFOREST WALK, CLAYTON, VIC 3800, AUSTRALIA

Email address: ricardo.ruizbaier@monash.edu

		h			
	κ	2^{-2}	2^{-3}	2^{-4}	2^{-5}
$\mathcal{B}_1$	10^{-9}	1.2 (5)	1.2 (1)	1.2 (1)	1.2 (1)
	10^{-4}	1.2 (6)	1.2 (6)	1.2 (6)	1.2 (6)
	1	1.2 (6)	1.2 (6)	1.2 (6)	1.2 (6)
	10^{4}	1.2 (6)	1.2 (6)	1.2 (6)	1.2 (6)
	10^{9}	1.2 (1)	1.2 (1)	1.2 (1)	1.2 (1)
$\mathcal{B}_2$	10^{-9}	3.7 (23)	4.1 (31)	4.4 (33)	4.5 (33)
	10^{-4}	3.6 (25)	3.8 (29)	3.5 (30)	3.5 (32)
	1	1.2 (11)	1.2 (11)	1.2 (11)	1.2 (11)
	10^{4}	1.0 (4)	1.0 (4)	1.0 (4)	1.0 (4)
	10^{9}	1.0 (3)	1.0 (3)	1.0 (3)	1.0 (3)

TABLE 4.4. Condition numbers (with MINRES iterations in parentheses) for different mesh sizes h and permeability κ for preconditioners $\mathcal{B}_1$ (schur complement) and $\mathcal{B}_2$ (weighted duality map corresponding to the weighted norms).